Phage Display and Peptide Mapping of an Immunoglobulin Light Chain Fibril-Related Conformational Epitope†

Brian O'Nuallain, Amy Allen, Demet Ataman, Deborah T. Weiss, Alan Solomon,* and Jonathan S. Wall

Human Immunology and Cancer/Alzheimer's Disease and Amyloid-Related Disorders Research Program, Department of Medicine, University of Tennessee Graduate School of Medicine, Knoxville, Tennessee 37920

Received June 26, 2007; Revised Manuscript Received August 7, 2007

ABSTRACT: Amyloid fibrils and partially unfolded intermediates can be distinguished serologically from native amyloidogenic precursor proteins or peptides. In this regard, we previously had reported that mAb 11-1F4, generated by immunizing mice with a thermally denatured variable domain (V_L) fragment of the human κ4 Bence Jones protein Len, bound to a non-native conformational epitope located within the N-terminal 18 residues of fibrillar, as well as partially denatured, Ig light chains (O'Nuallain, B., et al. (2006) *Biochemistry 46*, 1240−1247). To define further the antibody binding site, we used random peptide phage display and epitope mapping of V_L Len using wild-type and alanine-mutated Len peptides where it was shown that the antibody epitope was reliant on up to 10 of the first 15 residues of protein Len. Comparison of V_κ and V_λ N-terminal germline consensus sequences with protein Len and 11-1F4-binding phages indicated that this antibody's cross-reactivity with light chains was related to an invariant proline at position(s) 7 and/or 8, bulky hydrophobic residues at positions 11 and 13, and additionally, to the ability to accommodate amino acid diversity at positions 1−4. Sequence alignments of the phage peptides revealed a central proline, often flanked by aromatic residues. Taken together, these results have provided evidence for the structural basis of the specificity of 11-1F4 for both κ and λ light chain fibrils. We posit that the associated binding site involves a rare type VI β-turn or touch-turn that is anchored by a *cis*-proline residue. The identification of an 11-1F4-related mimotope should facilitate development of pan-light chain fibril-reactive antibodies that could be used in the diagnosis and treatment of patients with AL amyloidosis.

The amyloidoses are a group of over 20 protein misfolding disorders associated with often fatal sporadic and hereditary disorders, including Alzheimer's disease, type II diabetes, and primary (AL^1) amyloidosis (*1*−*4*). All types of amyloid, regardless of amino acid sequence, share tertiary structural and tinctorial features, i.e., they are formed from fibrils composed of extended β-sheets oriented perpendicularly to the long fibril axis (*5*, *6*) and bind the dyes thioflavin T and Congo red (*7*, *8*). Additionally, fibrils, as well as their assembly intermediates, contain generic conformational epitopes not present on the native proteins (*9*−*16*). These common characteristics reflect a similar fibrillogenic pathway-(s) involving the assembly of soluble higher-order intermediates into fibrils that are structurally dissimilar to their precursors (*2*, *13*, *17*).

Recently, we determined that the murine mAb 11-1F4, generated by immunizing mice with a thermally denatured variable region (V_L) fragment of the human κ4 Bence Jones protein Len (*18*), bound a cryptic, non-native epitope located within the first 18 residues of Ig light chains (LC) (*15*, *19*) (Figure 1). This antibody has shown therapeutic efficacy in a mouse model, as demonstrated by its ability to accelerate the removal of induced human AL amyloidomas, an effect that was independent of the κ or λ LC isotype or V_L subgroup of the injected fibrils (*12*). Additionally, mAb 11-1F4 inhibited *de novo* V_L fibrillogenesis (*19*).

Using random peptide phage display (*20*, *21*) and epitope mapping with wild-type and alanine mutated (*22*) Len peptides, we now have defined the nature of the epitope recognized on LC fibrils by mAb 11-1F4. Through phage peptide mimetics, as well as the discovery of a mimotope of 11-1F4's fibril-related epitope, we have shown that this cross-reactivity involves 10 of the first 15 LC residues. Additionally, our findings indicate that the 11-1F4 conformational epitope involves a rare type VI β-turn or touch-turn that is anchored by a *cis*-proline residue.

MATERIALS AND METHODS

Proteins, Peptides, and Antibodies. Recombinant (r) V_κ4 Len and V_λ6 Wil were produced in *Escherichia coli*, as previously described (*23*). The lyophilized proteins were dissolved in distilled water (∼1 mg/mL, ∼80 μM), 10× PBS

† This work was supported in part by the University of Tennessee Medical Center's Physicians Medical Education and Research Foundation, a NIBIB/NINDS Bioengineering Research Partnership Award EB 00789, USPHS Research Grant CA 100506 from the National Cancer Institute, and the Aslan Foundation. A.S. is an American Cancer Society Clinical Research Professor.

* To whom correspondence should be addressed. Tel: 865-544-9167. Fax: 865-544-6865. E-mail: asolomon@mc.utmck.edu.

[1] Abbreviations: Aβ, amyloid β peptide consisting of the first 40 amino acids; AL amyloidosis, light chain-associated amyloidosis; LC, light chain; EuLISA, europium (Eu^{3+})-linked immunosorbant assay; mAb, monoclonal antibody; PBSA, phosphate buffered saline containing 0.05% sodium azide; ThT, thioflavin T; V_L, light chain variable region.

10.1021/bi701255m CCC: $37.00
Published on Web 10/18/2007

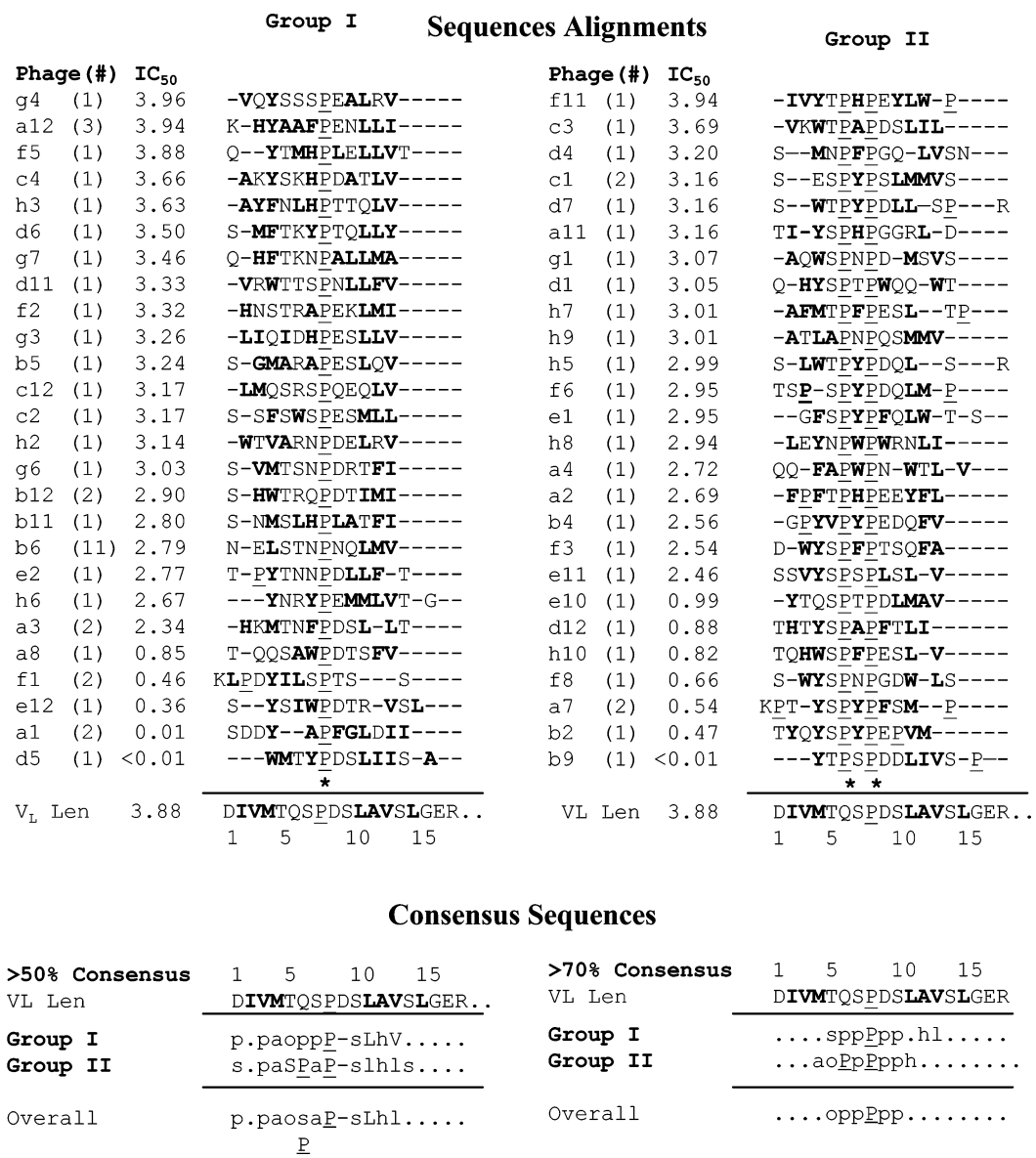

FIGURE 1: Multiple sequence alignments and consensus sequences for 11-1F4-binding phage peptides. Phage peptides were aligned (*28*) and divided into groups I and II, based on the presence of one of the two proline (-X-Pro-X- and Pro-X-Pro) or cysteine (Ile/Leu-Cys and Ile/Leu-X-Cys-) motifs, and each group adjusted to give the best alignment with the N-terminal sequence of V_L Len. The hydrophobic and/or aromatic residues are bolded and prolines underlined. Phage peptide consensus sequences were determined using the program CONSENSUS (http://www.bork.embl-heidelberg.de/Alignment/). Abbreviations include the following: a, aromatic (F, H, Y, W); h, hydrophobic, (A, C, F, I, L, M, V); l, aliphatic (I, L, V); o (S or T); p, polar (D, E, G, H, K, N, P, Q, R, S, T, W, Y); s, small side chain (A, C, D, G, N, P, S, T, V) (*31*); and each uppercase letter represents the particular amino acid.

containing 0.5% sodium azide (PBSA) was added to yield a concentration of 1×, and the samples passed through a 0.22 μm PVDF 25 mm Millex-GV syringe-driven filter unit (Millipore, Beillerica, MA). For competition studies, the proteins were centrifuged at 100000*g* for 2 h at room temperature. Protein concentrations were determined spectrophotometrically using 24,535 and 13,075 M^{-1} cm^{-1} as the E_{280}s for the Len and Wil proteins, respectively (ProtParam; http://us.expasy. org/tools/protparam.html); the final solutions were aliquoted and stored at −20 °C.

Synthetic phage and peptides encompassing all (or part) of the first 22 residues of Len were obtained from the Keck Biotechnology Center at Yale University (http://info.med.yale.edu/wmkeck/; New Haven, CT). Additionally, a peptide consisting of the first 15 Len residues, designated Len(1−15), was purchased from Sigma-Aldrich (St. Louis, Missouri). A custom Len(1−18) peptide library containing single alanine point mutations was generated by solid-phase synthesis at Mimotopes (Raleigh, NC), and the Aβ40 peptide was obtained from Quality controlled Biochemicals (Hopkinton, MA). Mass spectrometric analyses revealed the purity of the phage and Len preparations to be ∼50% and that of the Aβ40 peptide, >90%.

Before use, each lyophilized peptide was disaggregated by sequential exposure to TFA and HFIP, as described previously (*15*, *24*). After removal of the organic solvents by evaporation under argon, they were dissolved (0.25−1 mg/mL) in distilled water or 2 mM NaOH (depending on the p*I*) and 10× PBSA added to a final concentration of 1×. Prior to use, peptides from the Len(1−18) library were diluted from dimethylfluoride into PBSA. Len and phage samples were centrifuged at 20800*g* for 20 min at room temperature and Aβ at 50000*g* for 18 h at 4 °C. The concentration of peptide in each supernatant was determined,

based on a BSA standard curve, in a bicinchoninic acid colorimetric assay (micro-BCA, Pierce, Rockford, IL). Aβ samples were used immediately; Len and phage peptide preparations were stored at −4 °C for up to 48 h.

Bioreactor generated murine mAb 11-1F4 was furnished by the National Cancer Institute's Biopharmaceutical Development Program (SAIC-Fredrick, Inc., Fredrick, MD) and its concentration determined (E_{280}, 1.4 M^{-1} cm^{-1}).

Preparation of Amyloid Fibrils. Fibrils composed of $rV_\kappa 4$ Len and $rV_\lambda 6$ Wil were generated from filtered, soluble precursor proteins by agitation in an orbital shaker, as previously described (*25*). Briefly, 80 μM of protein in PBSA was placed in a closed 15 mL volume polypropylene tube which was shaken at 225 rpm at 37 °C. Aβ fibrils were generated by incubating the soluble precursor peptide at a concentration of ~30 μM in PBSA at 37 °C, as previously described (*14*). Maximum fibril formation occurred within 2 weeks, as evidenced by ThT fluorescence (*26*, *27*), after which the components were harvested by centrifugation (20800*g* for 25 min), sonicated, and stored at −20 °C.

Antibody Production and Characterization. BALB/c mice were immunized ×5 with 50 μg injections of an 11-1F4-binding synthetic phage peptide, designated a12 (NH_2-KHYAAFPENLLI-$CONH_2$), and conjugated via 1-ethyl-3-[3-dimethylaminopropyl] carbodiimide HCl to keyhole limpet hemocyanin (Pierce). The reactivity of sera obtained 1 week after the final injection against microtiter plate-immobilized a12 peptide, V_L fibrils, and collagen (Sigma) was determined in a europium (Eu^{3+}) based immunosorbant assay (EuLISA) (*15*, *16*), using both biotinyl-goat anti-mouse IgG and anti-IgM for detection.

Selection of 11-1F4 Binding Phage. To remove phage-containing 12-mer peptides that potentially bound nonspecifically to mAb 11-1F4, the Ph.D.-12 phage-display library (New England Biolabs) was preabsorbed with the murine monoclonal IgGκ protein MOPC-31C (Sigma). Briefly, 200 μL of 2 × 10^{11} unamplified phage was mixed for 4 h at room temperature with 50 μL of ~20 μg MOPC-31C attached to blocked (PBS containing 0.5% BSA) protein G magnetic beads. The resultant phage complexes were pelleted using a 6-tube magnetic separation rack (New England Biolabs) and the amount of unbound phage in the supernatant (60% recovery) determined by standard plaque titering procedures (*29*).

Isolation of 11-1F4-bound phage from the absorbed library was achieved by 4 rounds of biopanning. The selection process involved alternating the antibody binding protein (Protein G or A) and the blocking agent (0.5% BSA vs 1% gelatin in PBS) on the magnetic beads. Antibody-bound phage was eluted using the 11-1F4-binding Len(1−30) peptide (*15*, *16*). The first round consisted of gentle mixing and incubation of 25 nM antibody with 1.2 × 10^{11} absorbed phage in 0.3 mL of PBS containing 0.05% Tween 20 (PBST) for 1 h at room temperature. The sample then was added to 50 μL of protein G beads blocked with 0.5% BSA, and, after incubation, the beads were washed ×10 with 1 mL of PBST; 11-1F4-bound phage was eluted with 3 μM Len(1−30) in 0.3 mL of PBST and then amplified from 3.9 × 10^6 to ~3 × 10^{13}, using standard amplification and plaque titrating procedures (*28*). An aliquot (1.2 × 10^{11}) of the amplified phage was used to pan against 11-1F4 bound to gelatin-blocked protein A beads. After 2 additional steps, the antibody-reactive phage were stored in 20% glycerol at −20 °C for up to 6 months, with no observable loss in antibody reactivity.

Isolation and Sequencing of Clonal Phages. For phage plaque hybridization, a Protran BA85 0.45 μm nitrocellulose membrane (Schleicher and Schuell), soaked in transfer buffer (PBST), was placed on top of an LB/IPTG/Xgal agar plate containing ~100 plaques and incubated at 37 °C for 1 h. The membrane was lifted and blocked with assay buffer (0.5% gelatin in PBS containing 1% Tween 20), unbound blocking agent removed, and 30 nM of mAb 11-1F4 added. After incubation and washing ×3 with PBST, HRP-labeled goat anti-mouse IgG antibody (Jackson Immunoresearch Labs, West Grove, PA) was added and, after washing, phage-bound 11-1F4 was detected by chemiluminescence using ECL (Amersham Biosciences Corp., Piscataway, NJ) as the substrate. An 11-1F4 binding phage plaque was defined by the presence of a strong positive signal detected on duplicate hybridizations. In total, 96 positive plaques were picked, amplified, and phage DNA-purified using a QIAprep Spin M13 Kit (QIAGEN Inc., Valencia, CA). Sequencing was performed with an ABI PRISM 3100 Genetic Analyzer (Applied Biosystems, Foster city, CA) with a Big Dye v3.0 Cycle Sequencing kit (Applied Biosystems) at the University of Tennessee's Molecular Biology Resources Facility. Phage peptide sequences were aligned using CLUSTALW (*28*).

11-1F4 Binding and Competition Assays. The relative strength of mAb 11-1F4 binding with clonal phage, peptides, and rV_L Len was determined by EuLISA (*15*, *16*) in the presence or absence of NaSCN (*30*). The NaSCN assay involved coating 5 × 10^{10} phage (as determined from A_{269nm} (*29*)) in PBS onto each well of a high-binding microtiter plate (EIA/RIA Easy Wash, COSTAR, Corning, NY) which was covered and incubated overnight at 37 °C. The plate was washed ×3 with PBST, blocked with 1% BSA in PBS, and a solution of 1 nM 11-1F4 in assay buffer (blocking buffer containing 0.05% Tween 20) added. After a 1 h incubation and a washing step, 0−7 M NaSCN in 50 mM phosphate, pH 7.5, was added and the plate incubated for 15 min at 37 °C, followed (after washing) by sequential addition of biotin-labeled goat anti-mouse IgG (Sigma), Eu^{3+}-streptavidin conjugate (Perkin-Elmer), and low-pH Eu^{3+} releasing enhancement solution (Perkin-Elmer) (*15*). For Len and phage peptide competition EuLISAs, up to 1 mM polypeptide competitor in solution with 2 nM 11-1F4 mAb was included. In the case of Jto and Aβ40, these analyses involved preincubation of 500 nM 11-1F4 with ~0.2 mg/mL competitor for 40 min at 37 °C.

All microtiter plate experiments were done in triplicate in assay buffer (1% BSA in PBS containing 0.05% sodium azide and 0.05% Tween 20). Immediately prior to immobilization, amyloid fibrils and collagen stocks were sonicated (2 × 30 s bursts) with a probe sonic disruptor (Teledyne/Tekmar, Mason, OH). The error bars in figures represent SD. Values for EC_{50} and IC_{50} were determined from sigmoidally fit antibody binding curves (SigmaPlot 2000 ver. 6; Systat Software, Inc.).

RESULTS

Phage Peptides Have Position-Specific Sequence Identity with V_L Len. Alignment of the amino acid sequence of V_L

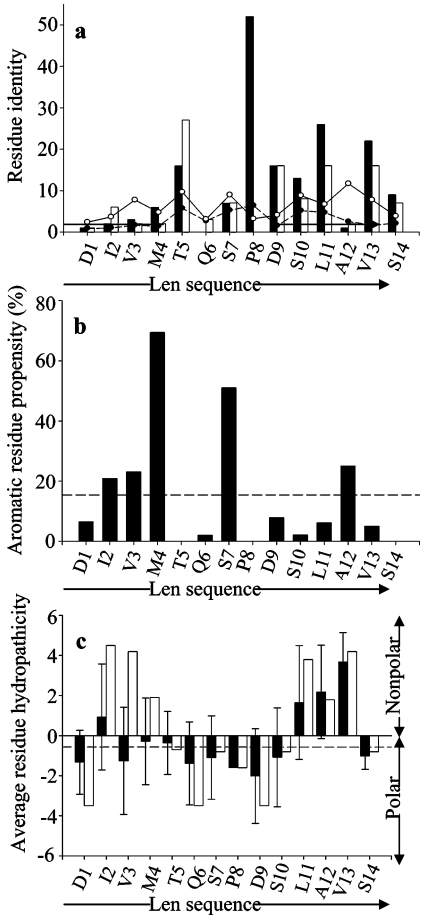

FIGURE 2: Sequence-position comparison of 11-1F4-binding phage peptides with the first 14 residues of V_L Len. (a) Residue identity between phage peptides and V_L Len; the numbers of identical (closed bars) and chemically similar (open bars) residues for each position are shown. The solid and open circles indicate the number of identical and chemically similar phage peptide residues expected to occur by chance, based on the observed frequency of amino acids in the random peptide phage display library (http://www.neb.com/nebecomm/ ManualFiles/manualE8110.pdf). (b) Percentage of aromatic residues in the phage peptides at each position. The line dashed represents the percentage abundance of aromatic amino acids relative to all other residues in the random peptide phage display library. (c) Average residue hydropathicity values (*32*) for phage peptides (closed bars) relative to those of the Len(1−14) peptide (open bars). Each sequence position average hydropathicity value was determined from the sum of residue hydropathicity values divided by the number of total residues. The dashed line shows the average hydropathicity value for all 20 amino acids, corrected for the abundance of each in the random peptide phage display library. All sequence-position comparisons were determined using the multiple sequence alignments shown in Figure 1.

Len with 11-1F4-binding phage peptides indicated that the epitope recognized by this mAb was located within the first 14 residues (Figure 1). With rare exception, the peptides contained at least 1 proline corresponding to Pro8 in V_L Len and one half had a second proline. Based on these results, 11-1F4-binding peptides were grouped into two families: -X-Pro-X- or -Pro-X-Pro- (Figure 1, groups I and II).

Analyses of consensus sequences for phage peptides assigned to group I or II (50% and 70% threshold values, respectively) showed that there was a high proportion of identical or physiochemically similar amino acids (*31*) at 10 of the first 14 positions of protein Len (Figures 1 and 2a), with maximum conserved identity occurring at positions 5, 8, 9, 11, and 13 (Thr, Pro, Asp, Leu, and Val, respectively). This correlation was greater than would be expected, based on the observed frequency of amino acids in the random peptide phage display library (http://www.neb.com/nebecomm/ManualFiles/ manualE8110.pdf). The overall consensus sequence, incorporating peptides from both groups I and II, revealed that the region of greatest homology spanned a 6-polar residue stretch between positions 5 and 10 (Figure 1). Similarity also was observed within the first 4 positions of the phage peptide sequences that contained a high percentage of aromatic resides at position 4; however, these amino acids were dissimilar to those found in the Len molecule (Figures 1 and 2a,b). Three additional positions—6, 7, and 12 (Gln, Ser, and Ala)—also exhibited considerable sequence heterogeneity, with a predominance of aromatic residues at position 7.

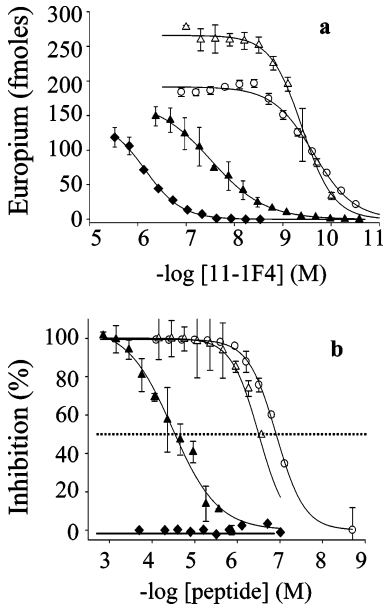

FIGURE 3: Binding of mAb 11-1F4 to plate-immobilized Len peptides. (a) Binding of 11-1F4 to Len peptides. (b) Competitive inhibition of 2 nM 11-1F4 binding to Len(1−22) in the presence or absence of Len peptides. Len(1−15) (△); Len(1−13) (▲); LenP8S(1−22) (◆); and Len(1−22) (○). The dashed line indicates 50% inhibition.

In contrast to V_L Len, the presence of more polar residues within the first 4 positions of the phage peptides resulted in a hydrophilic N-terminal (Figure 2c). Further characterization of their physiochemical properties, such as p*I*, electrostatic charge, stability, aliphaticity, and hydropathicity (http://us.expasy.org/cgi-bin/protparam), indicated that these molecules were more basic [p*I* values = 5.60 ± 1.5 vs 3.56 for Len(1−15)].

The 11-1F4 Epitope Is within the First 15 Residues of V_L Len. mAb 11-1F4 bound equally to plate-immobilized V_L Len and Len peptides encompassing the first 15 residues, with EC_{50} values in the subnanomolar range (Figure 3a, Table 1). In contrast, the reactivity of 11-1F4 with Len(1−13) was ∼50× weaker, thus indicating the importance of Ser14 and/or Leu15 for this interaction. Consistent with these observations, both the Len(1−22) and Len(1−15) peptides were similarly effective at inhibiting 11-1F4 binding to plate-immobilized Len(1−22), whereas Len(1−13) was ∼30× less effective (Figure 3b, Table 1).

Table 1: 11-1F4 Binding to Plate Immobilized Phage and Len Peptides and the Inhibitory Effects of These Molecules on Antibody Binding to Immobilized Len(1−22)

			immobilized polypeptide		
polypeptide	phage peptide group[a]	sequence[b]	EC_{50}[c] (nM)	NaSCN assay IC_{50}[d] (μM)	solution-phase competition IC_{50}[e] (μM)
Len V_L	na[f]	D**IVM**TQSP*DS***LAVSL**G*ER***ATI**N...	0.18 ± 0.03	3.9	≫30
a12	I	*K*-**HYAAF**P*E*N**LLI**	0.54 ± 0.3	3.7 (3.9)	1.5 ± 0.1
g4	I	-**VQY**SSSP*E***AL***R***V**	14 ± 6.0	3.7 (4.0)	3.2 ± 0.0
f11	II	-**IVY**TP**H**P*E***YLW**-P	32 ± 0.1	3.3 (3.9)	6.7 ± 0.1
b2	II	T**Y**Q**Y**SP**Y**P*EP***VM**	44 ± 0.1	0.5 (0.5)	4.6 ± 0.1
a7	II	*K*PT-**Y**S**P****Y**P**F**S**M**--P	18 ± 0.1	2.3 (0.5)	1.7 ± 0.1
Len(1−22)	na	D**IVM**TQSP*DS***LAVSL**G*ER***ATI**N	0.24 ± 0.1	1.37	0.07 ± 0.01
Len(1−15)	na	D**IVM**TQSP*DS***LAVSL**	0.39 ± 0.05	nd[g]	0.27 ± 0.01
Len(1−13)	na	D**IVM**TQSP*DS***LAV**	16 ± 0.1	nd	33 ± 0.07

[a] Phage peptides were grouped based on the presence of highly conserved proline residues, as shown in Figure 1. [b] Peptide sequences were aligned by CLUSTALW (*28*); hydrophobic and/or aromatic residues are bolded, and proline is underlined. [c] Each EC_{50} value was determined from the midpoint of 11-1F4 titration curves, as shown in Figures 3a, 4c, and 5a. [d] Each IC_{50} value was determined from the midpoint of NaSCN titration curves (see Figure 4b). IC_{50} values with or without brackets were determined for 11-1F4 binding to phage peptides alone or expressed on phage particles, respectively. [e] Each IC_{50} value was determined from the midpoint of peptide competition curves shown in Figures 3b and 5b. [f] Not applicable. [g] Not determined. Charged residues are italicized.

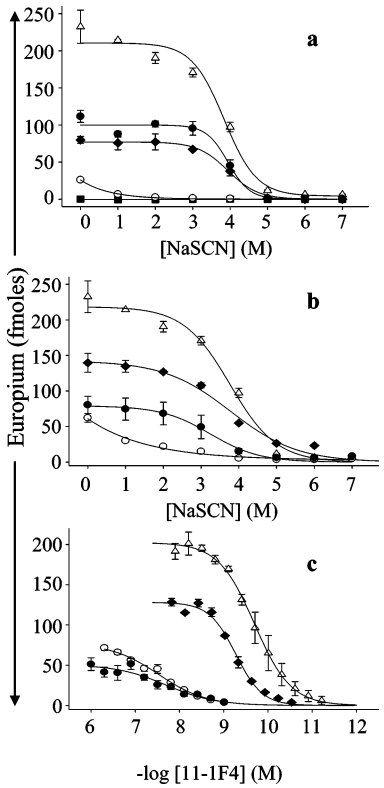

FIGURE 4: 11-1F4-binding to plate-immobilized phage, V_L Len, and synthetic phage peptides. NaSCN titration curves for antibody binding to (a) phage, protein Len, or (b) synthetic phage peptides and Len. (c) 11-1F4 titration curves for binding to synthetic phage peptides and Len. IC_{50} and EC_{50} values were determined from the midpoint of each titration curve. Len (△); f11 (●); b2 (○); and a12 (◆) phage particles or peptide; and unamplified phage display library control (■).

11-1F4 Binding to Non-Native V_L Len, Len LC, Len Peptides, and Phages. A broad range of IC_{50} values (0.5−<0.01 M) were obtained when ∼50 11-1F4-binding phages were evaluated (Figure 1). Notably, the strongest antibody complexes (IC_{50}, ∼4 M) occurred with phages a12, f11, c3, c4, g4, f5, and h3 (Figures 1 and 4a). In contrast, the b2 phage and several others that were isolated based on positive interactions with the antibody bound weakly in the presence of NaSCN. As expected, no or very weak binding was observed with polyclonal phages from the unselected library. Presumably, the lower assay signal that was found for 11-1F4 binding to the immobilized phage (as compared to that for protein Len) reflected differences in epitope density that resulted from antigen immobilization.

To confirm that mAb 11-1F4 reactivity with the phage was *via* the 12-mer peptide mimetics expressed on its surface, synthetic peptides representing high-affinity (a12, g4, and f11) or weak binding (b2 and a7) phage were tested in the NaSCN assay. With the exception of the a7 molecule, the antibody reacted with the isolated peptides in a fashion similar to that of the entire phage. Three—a12, g4 and f11—bound the mAb 11-1F4 in the presence of ∼3.5 M NaSCN, comparable to that seen when V_L Len was used as substrate (Figure 4a,b, Table 1). In contrast, the a7 synthetic peptide interacted with 11-1F4 at much greater concentrations of chaotrope, as compared to the phage-expressed a7 derivative (IC_{50}, 2.3 M vs 0.54 M), indicating an increase in stabilizing hydrophobic and/or electrostatic interactions between the antibody and the synthetic peptide (Table 1).

Consistent with results obtained using the NaSCN-titration assay, antibody binding curves showed that mAb 11-F4 bound with similar affinity to both the a12 synthetic peptide and V_L Len with EC_{50}s of 0.5 and 0.2 nM, respectively (Figure 4c). However, antibody binding to the a7, g4, and f11 synthetic peptides was much weaker than with the respective phage and was comparable to the interaction with the b2 peptide that formed a relatively weak complex with 11-1F4 in the presence of NaSCN (Figure 4c, Table 1). Presumably, these assay-related discrepancies reflect differences in the methods used to measure antibody binding.

To ascertain if the epitope recognized by mAb 11-1F4 was retained when the synthetic phage peptides were in solution, their ability to inhibit the reactivity of 11-1F4 with plate-immobilized Len(1−22) was determined. These studies showed that each had a similar capacity with IC_{50}s in the 1.5−6.7 μM range (Figure 5, Table 1), values ∼20-fold higher than that for Len(1−22); in contrast, the native protein Len failed to suppress the reaction (IC_{50}, > 30.0 μM).

Alanine Scanning Mutagenesis. The substitution of alanine for proline, asparagine, leucine, or valine at positions, 8, 9, 11, and 13, respectively, markedly hindered the interaction

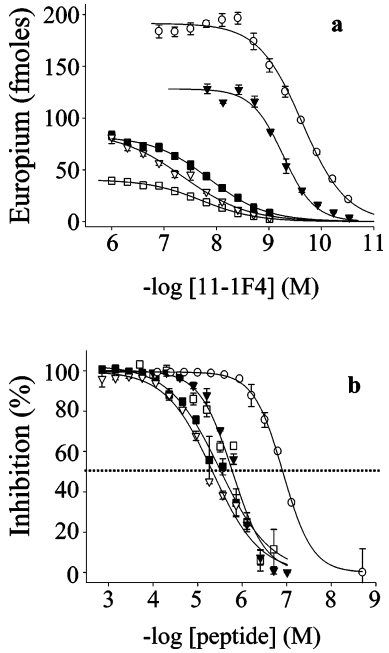

FIGURE 5: Binding of mAb 11-1F4 to plate-immobilized Len(1−22) and phage peptides in the presence and absence of peptide inhibitors. (a) Binding of 11-1F4 to phage peptides or Len(1−22). (b) Competitive inhibition of 2 nM 11-1F4 binding to Len(1−22) in the presence of phage peptides or Len(1−22). The dashed line indicates 50% inhibition. a12 (▼); g4 (■); b2 (▽); a7 (□); and Len(1−22) (○).

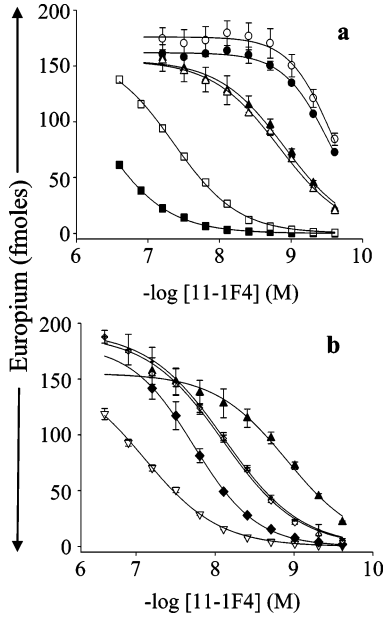

FIGURE 6: Interaction of mAb 11-1F4 with plate-immobilized, Ala-substituted Len(1−18) peptides. (a) Binding of 11-1F4 to Len(1−18) (▲); IA2 (○); V3A (●); T5A (△); D9A (□); and P8A (■). (b) Antibody binding to Len(1−18) (▲); I11A (▽); V13A (◆); S14A (◇); and I15A (×).

of the Len(1−18) with mAb 11-1F4, yielding ∼20−400-fold higher EC_{50} values (Figure 6, Table 2). The greatest effect was observed with Pro8Ala. These results were consistent with the significant sequence identity that occurred at these 4 positions in the phage peptides and V_L Len, as well as our previous finding that 11-1F4-binding to Len peptides was drastically reduced by the substitution of serine for proline at position 8 (*15*). In addition, the relatively large

Table 2: Peptide Phage Display and Alanine Scanning Analysis of N-Terminal V_L Len Residues Implicated in 11-1F4 Binding

V_L Len residue position	phage peptide identity[a] (%)	phage peptide Ala (%)	Len(1−18) alanine scanning EC_{50}[b] (nM)	Len(1−18) alanine scanning EC_{50} WT EC_{50}[c]	phage and Len(1−18) residue preferences[d]
D1	3.8	0	3.91 ± 0.001	2.7	S or T
I2	15.4	19.2	0.27 ± 0.001	0.22	Ala or any amino acid
V3	9.6	0	0.29 ± 0.004	0.24	polar
M4	15.4	0	2.51 ± 0.01	2.1	aromatic (preferably Tyr)[e]
T5	82.7	10.0	1.48 ± 0.01	1.2	small (preferably S or T)
Q6	5.8	4.0	2.33 ± 0.01	1.9	polar
S7	26.9	8.0	0.62 ± 0.01	0.51	polar (preferably aromatic)
P8	100	0	>500 ± 10	>400	invariant proline
D9	61.5	2.0	43.2 ± 0.2	36	negatively charged, D/E
S10	40.4	6.3	0.85 ± 0.003	0.71	small polar (preferably S or T)
L11	80.8	0	77.1 ± 0.7	64	L or bulky hydrophobic
A12	5.8	0	2.86 ± 0.02[d]	2.4	bulky hydrophobic
V13	73.0	2.6	18.6 ± 0.1	16	V or aliphatic
S14	30.7	0	7.96 ± 0.04	6.6	S or T
L15	na[f]	na	7.64 ± 0.02	6.4	(L)
G16	na	na	2.12 ± 0.01	1.8	na
E17	na	na	2.48 ± 0.01	2.1	na
R18	na	na	0.55 ± 0.002	0.5	na

[a] Sequence identity for each phage peptide compared to V_L Len was determined as the sum of the percentages of identical and chemically similar (*31*) residues at each position from the multiple sequence alignments of phage peptide groups I and II shown in Figure 1. [b] EC_{50} values were determined from the midpoint of 11-1F4 titration curves shown in Figure 6. [c] WT EC_{50} is the EC_{50} value for 11-1F4 binding to plate-immobilized wild-type Len(1−18). [d] Residue preference at each position in Len(1−18) was determined from the multiple sequence alignments of phage peptide groups I and II with V_L Len, and the binding of 11-1F4 to Ala-substituted Len(1−18) peptides (Figures 1, 2, and 6). Residue preferences with or without brackets are those that were preferred for Len and phage peptides, respectively. [e] Residue preferences in brackets are those specific to the Len(1−18) peptide. [f] Not applicable.

decrease in antibody binding with Asp9Ala, Leu11Ala, and Val13Ala substitutions correlated with the lack of an alanine residue at these corresponding positions in the phage peptides (Table 2).

The substitution of alanine for any of the first 4 residues of Len(1−18) had little effect on 11-1F4 binding (Table 2); however, stronger interactions occurred with the Ile2Ala and Val3Ala variants that generated EC_{50} values ∼4× greater than that for the wild-type peptide (Figure 6, Table 2). Increased antibody binding to the Ile2Ala variant was in agreement with the frequent occurrence (19.2%) of alanine at this position in the phage peptides (Table 2). In contrast, alanine was never observed in the location equivalent to Val3. Instead, polar residues were abundant, including a high percentage of aromatic amino acids (Table 2), thus suggesting that these differences reflected variations in side-chain usage for maintaining the conformational epitope recognized by 11-1F4 in the Len and the phage-derived peptides.

Several other variations were observed between the Ala scanning and phage peptide alignment analyses (Table 2). The Leu15Ala substitution in Len(1−18) resulted in ∼6× weaker peptide interaction with 11-1F4, implying an important role of leucine for this reactivity; however, this residue was absent at this position in the 11-1F4 binding phage peptides (Figure 1). In addition, the Thr5Ala and Ser10Ala substitutions in Len(1−18) had little effect on antibody binding, although there was a preference for hydroxyl side chains at these positions in the phage peptides (Figures 2 and 6, Table 2).

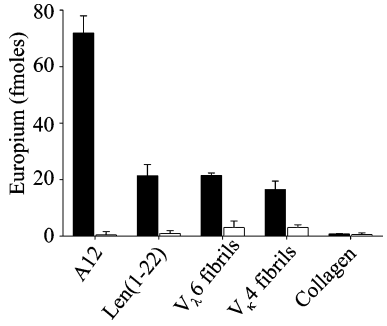

FIGURE 7: Characterization of the specificity of anti-phage peptide immune serum. Reactivity of serum from an a12-immunized mouse (solid bars) and nonimmunized mouse (open bars) against the immunogen, Len(1−22), as well as V_L fibrils, and collagen fibrils.

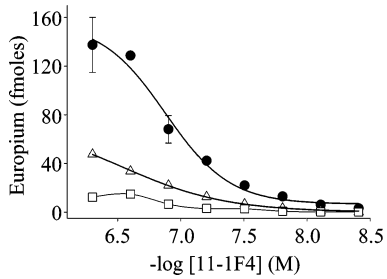

FIGURE 8: Competitive inhibition of mAb 11-1F4 binding to Aβ40 fibrils. Binding of antibody to plate-immobilized Aβ40 fibrils in the absence of competitor (●) or in the presence of Jto fibrils (□) or Aβ40 fibrils (△). Competition experiments were performed by preincubating 11-1F4 with ∼0.2 mg/mL fibrils.

Immunizing Mice with the a12 Peptide Generated Anti-Light Chain Fibril Antibodies. To validate that the phage peptides mimicked the structure of the fibril-associated epitope recognized by 11-1F4, mice were immunized with KLH-conjugated a12 peptide. The resultant immune sera contained antibodies that had reactivity similar to that for mAb 11-1F4; namely, they had specificity for the a12 and Len(1−22) peptides, as well as synthetic fibrils composed of V_λ6 Wil and V_κ4 Len (Figure 7). Neither 11-1F4 nor the a12-immune serum recognized non-amyloid triple-helix collagen fibrils. In addition, sera from nonimmunized mice were virtually unreactive with the test molecules.

11-1F4 Binding to Aβ40 Fibrils. The reactivity of mAb 11-1F4 with Aβ40 fibrils was demonstrated by EuLISA. As shown in Figure 8, the EC_{50} of this interaction was ∼100 nM, a value comparable to that obtained with LC fibrils (*15*). To determine if the binding could be inhibited by LC fibrils, we carried out competition studies where we found that sonicated V_λ6 (Jto) and Aβ40 fibrils, at 50-fold excesses, were equally potent as inhibitors, indicating that the antibody used the same paratope for binding to heterologous fibrils.

DISCUSSION

The aggregation of amyloidogenic proteins into insoluble fibrils is associated with a series of conformational transitions that result in the exposure of neo-antigenic sites that are associated with amyloid fibrils and assembly intermediates (*10*−*14*, *16*, *31*, *33*, *34*), as well as the loss of native epitopes (*35*, *36*). We previously had demonstrated that mAb 11-1F4 bound to a cryptic epitope present on κ and λ LC amyloid fibrils, as well as partially denatured precursor proteins, but did not when these proteins were in their native state (*15*, *19*). Using overlapping peptide mapping techniques, the epitope was localized within the first 18 amino acids of the V_κ4 Len immunogen. We hypothesized that the LC fibril binding site involved an edge-strand perturbation, similar to the neo-epitope formed by TTR fibrils (*37*). Additionally, the requirement of Pro8 (conserved within virtually all κ and λ LCs (*38*, *39*)) for this interaction to occur led to our postulation that this residue anchored a β-turn and led to a peptide chain reversal, analogous to that formed from *trans*-proline in β2-microglobulin fibrils (*40*, *41*). To understand more fully the molecular basis of mAb 11-1F4's reactivity with both κ and λ LCs, as well as the nature of the fibril-specific epitope recognized by this reagent, we probed the structural characteristics of this determinant using peptide phage display and peptide epitope mapping.

Our studies indicated that 11-1F4 binding to V_κ4 Len and non-κ4 light chains was reliant on an invariant proline and up to 9 other residues (Asp1, Ile2, Val3, Met4, Asp9, Leu11, Val13, Ser14, and Leu15). We attribute the stronger 11-1F4 interactions with κ4 fibrils, as compared with those formed from other LC isotypes (EC_{50}s, 0.2 nM vs ∼ 100 nM, respectively (*15*)), to the presence of an Asp at position 9, given that the single germline gene that encodes V_κ4 proteins specifies this amino acid at this location (*38*); additionally, the Asp9 substitution in Len(1−18) resulted in a 60-fold weaker antibody binding with an EC_{50} value similar to that for non-κ4 LCs. Further, ∼60% of the 11-1F4-binding phage peptides contained a negatively charged amino acid (Asp or Glu) at position 9.

Inspection of germline V_κ and V_λ N-terminal consensus sequences revealed identity, compared to V_κ4 LCs, at 9 positions (1, 4, 5, 6, 8, 10, 11, 12, and 14) that we had implicated in mAb 11-1F4 binding (Figure 9a). Notably, this antibody reacts with similar affinity to all non-κ4 AL fibrils, partially denatured LCs, and non-LC fibrils (*12*, *15*). Presumably, this reflects an ability to accommodate significant side-chain diversity within the 11-1F4 binding site that we attribute to an unusually large pocket resulting from an uncommonly short (i.e., 2-residue) heavy chain CDR3 (C. Dealwis and A.S., unpublished data).

Phage display analyses and alanine-scanning mutagenesis of the Len(1−18) indicated that mAb 11-1F4 specificity depended primarily on the presence of an invariant prolyl residue at position(s) 7 and/or 8. The requirement of a ubiquitous proline for 11-1F4 binding is unlikely to be due to direct interaction with this residue, since the antibody does not recognize proline-rich collagen (*15*) (Figure 7). Antibody binding also was highly dependent on the presence of a leucine and valine at positions 11 and 13, respectively. Notably, there were high numbers of Leu11 and Val13 within the 11-1F4-binding phage peptides and these residues also are specified by V_κ2, V_κ4, and V_λ7 germline genes (*38*).

Although all κ LCs exhibit significant sequence identity with the first 4 residues of protein Len (a region important for 11-1F4 binding (*15*)), λ proteins are dissimilar. Nevertheless, these differences did not affect antibody reactivity since 11-1F4 bound equally to κ (non-κ4) and λ LCs (*15*). The ability of 11-1F4 to tolerate LC side-chain diversity within this region was demonstrated by the formation of stable antibody-phage complexes that occurred with phage peptides containing an N-terminal glutamine or serine (residues typically found in λ LCs, in contrast to aspartic or glutamic

a **N-terminal V_κ and V_λ consensus sequences**

	1 5 10 15
Vκ4	DIVMT QSPDS LAVSL
V_κ germline	DI.MT QSPuS LShSs
V_λ germline	pphLT QPP-S VSsuP

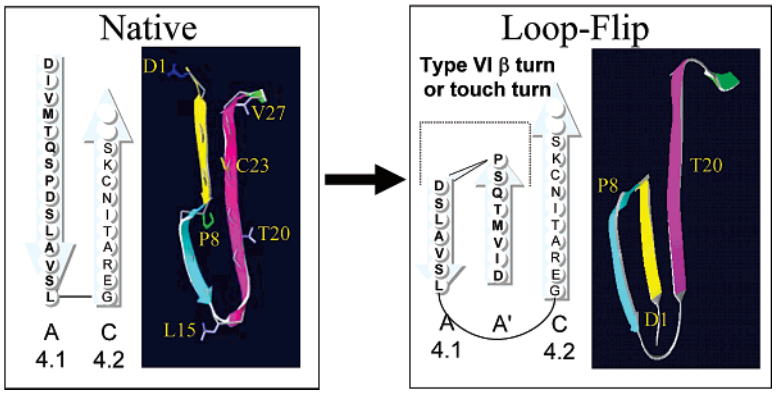

FIGURE 9: Consensus sequence analyses and schematic representation of the conformational fibril-associated epitope recognized by mAb 11-1F4. (a) Comparison of V_κ4 with non-κ4 germ line consensus sequences (bolded residues are hydrophobic.). Abbreviations used in consensus sequences are as follows: h, hydrophobic (A, C, F, I, L, M, V); p, polar (D, E, G, H, K, N, P, Q, R, S, T, W, Y); s, small residues (A, C, D, G, N, P, S, T, V); and u, minute residues (A, C, G, S). Consensus sequences were determined from V_L germline sequences using CONSENSUS (http://us.expasy.org/tools/) analysis of CLUSTALW (*28*) multiple aligned sequences with 70% threshold; prolines are underlined. (b) Proposed model for the conformational epitope recognized by 11-1F4 involves a rearrangement of the first 9 V_L residues centered on a *cis*-proline type VI β-turn or touch-turn induced by partial denaturation via surface adsorption or by fibrillogenesis. The N-terminal 15 residues are bolded.

acid common to κ proteins). Additionally, the presence of an aromatic amino acid at the third position in ~20% of the 11-1F4-binding phage peptides (and present in one-third of all λ proteins) indicates the capability of this antibody to accommodate side-chain diversity within this region.

Confirmation of the Structure of the Neo-Epitope Bound by 11-1F4. Based on X-ray crystallographic analysis of the V_L dimer Len (*42*), we posited that 11-1F4 bound a non-native structure present within the first 18 LC residues (*15*) and that this interaction required a peptide chain reversal that moved a portion of strand A (4.1) adjacent to strand B (4.2), following the formation of a Pro8-anchored type I or *cis*-Pro8 type VI-β turn (*43*) or touch-turn (*44*). In native LCs, these residues are involved in β-sheet formation and, further, a *cis*-Pro8 anchors an open turn or bend within strand A (Figure 9b); thus, a chain reversal would reposition the first 4 residues, shown to be critical for maintaining antibody-binding, in close proximity to the equally essential amino acids between positions 11 and 15.

The phage peptide analyses provide further support for a β-turn epitope, as evidenced by the characteristic distribution of amino acids next to the ubiquitous central prolyl residue. Such turns generally consist of a stretch of polar residues flanking a central proline(s) which, in turn, is bordered on either side by amino acids frequently found in the β-strands of β-hairpin peptides (*45*, *46*). Additionally, the clustering of aromatic and hydrophobic residues at the N- and C-termini of the phage peptides presumably provides the driving force for β-hairpin folding (*47*). Our experimental data also indicate that the epitope is likely to be anchored by a type VI β-turn or touch turn, since the unusually high propensity for an aromatic residue to precede the central proline in the phage peptides is consistent with a *cis*-proline conformation (*48*−*50*). Additionally, the large decrease in 11-1F4 binding that occurred with the substitution of proline for alanine at position 8 of Len(1−18) is consistent with a *cis*-proline β-turn, as such a dramatic effect would not occur in β-turns anchored by a *trans*-prolyl residue (*43*, *44*). The presence of 2 adjacent prolines, which are found in rare type VI β-turns (*51*−*53*), also was seen in ~50% of all phage peptide sequences and occurs in the majority of proteins encoded by V_λ genes. We posit that mAb 11-1F4's unusually large binding pocket enables interaction with Aβ fibrils, which, although lacking a prolyl residue, putatively contain a type I β-turn (*54*).

Generation of Pan-LC Fibril-Reactive Antibodies Using the a12 Mimotope. The finding that the a12 peptide is a mimotope (*55*) (i.e., induced a murine antibody response that mimicked 11-1F4 cross-reactivity) suggests that this molecule may serve as a vaccine to generate therapeutic antibodies in patients with AL amyloidosis. Recently, phage peptide mimotopes also have been identified against conformational epitopes on Aβ42 fibrils (*56*); presumably, this class of molecules has several advantages over immunization with soluble or fibrillar amyloidogenic proteins, including enhanced immunogenicity compared to self-antigens and reduced toxicity. Additionally, it is more likely that a pan-LC fibril-reactive antibody response that is not biased toward a κ or λ isotype would be obtained using the a12 peptide.

Our future efforts will be devoted toward the generation of pan-LC fibril-reactive mAbs using the a12 immunogen and confirmation of the structure of the neo-epitope bound by mAb 11-1F4 through X-ray crystallographic studies of an 11-1F4-Len(1−15) complex, as well as determination of the solution structure of wild-type and chemically modified Len(1−15) (with stabilizers of the central *cis*-proline (*57*, *58*)) using CD, NMR, and/or FRET analysis. These studies should provide the necessary information for generation of novel reagents to be used as therapeutic and/or diagnostic tools in patients with AL amyloidosis.

REFERENCES

1. Comenzo, R. L. (2007) Current and emerging views and treatments of systemic immunoglobulin light-chain (Al) amyloidosis, *Contrib. Nephrol. 153*, 195−210.
2. Stefani, M. (2004) Protein misfolding and aggregation: new examples in medicine and biology of the dark side of the protein world, *Biochim. Biophys. Acta 1739*, 5−25.
3. Westermark, P., Benson, M. D., Buxbaum, J. N., Cohen, A. S., Frangione, B., Ikeda, S., Masters, C. L., Merlini, G., Saraiva, M. J., and Sipe, J. D. (2005) Amyloid: toward terminology clarification. Report from the Nomenclature Committee of the International Society of Amyloidosis, *Amyloid 12*, 1−4.
4. Ross, C. A., and Poirier, M. A. (2004) Protein aggregation and neurodegenerative disease, *Nat. Med. 10 Suppl.*, S10−S17.
5. Makin, O. S., Atkins, E., Sikorski, P., Johansson, J., and Serpell, L. C. (2005) Molecular basis for amyloid fibril formation and stability, *Proc. Natl. Acad. Sci. U.S.A. 102*, 315−320.
6. Makin, O. S., and Serpell, L. C. (2005) Structures for amyloid fibrils, *FEBS J. 272*, 5950−5961.
7. LeVine, H., 3rd. (1993) Thioflavine T interaction with synthetic Alzheimer's disease beta-amyloid peptides: detection of amyloid aggregation in solution, *Protein Sci. 2*, 404−410.
8. Westermark, G. T., Johnson, K. H., and Westermark, P. (1999) Staining methods for identification of amyloid in tissue, *Methods Enzymol. 309*, 3−25.
9. Dumoulin, M., and Dobson, C. M. (2004) Probing the origins, diagnosis and treatment of amyloid diseases using antibodies, *Biochimie 86*, 589−600.
10. Franklin, E. C., and Zucker-Franklin, D. (1972) Antisera specific for human amyloid reactive with conformational antigens, *Proc. Soc. Exp. Biol. Med. 140*, 565−568.
11. Glabe, C. G. (2004) Conformation-dependent antibodies target diseases of protein misfolding, *Trends Biochem. Sci. 29*, 542−547.
12. Hrncic, R., Wall, J., Wolfenbarger, D. A., Murphy, C. L., Schell, M., Weiss, D. T., and Solomon, A. (2000) Antibody-mediated resolution of light chain-associated amyloid deposits, *Am. J. Pathol. 157*, 1239−1246.
13. Kayed, R., Head, E., Thompson, J. L., McIntire, T. M., Milton, S. C., Cotman, C. W., and Glabe, C. G. (2003) Common structure of soluble amyloid oligomers implies common mechanism of pathogenesis, *Science 300*, 486−489.
14. O'Nuallain, B., and Wetzel, R. (2002) Conformational Abs recognizing a generic amyloid fibril epitope, *Proc. Natl. Acad. Sci. U.S.A. 99*, 1485−1490.
15. O'Nuallain, B., Allen, A., Kennel, S. J., Weiss, D. T., Solomon, A., and Wall, J. S. (2007) Localization of a conformational epitope common to non-native and fibrillar immunoglobulin light chains, *Biochemistry 46*, 1240−1247.
16. O'Nuallain, B., Hrncic, R., Wall, J. S., Weiss, D. T., and Solomon, A. (2006) Diagnostic and therapeutic potential of amyloid-reactive IgG antibodies contained in human sera, *J. Immunol. 176*, 7071−7078.
17. Kourie, J. I., and Henry, C. L. (2002) Ion channel formation and membrane-linked pathologies of misfolded hydrophobic proteins: the role of dangerous unchaperoned molecules, *Clin. Exp. Pharmacol. Physiol. 29*, 741−753.
18. Schneider, M., and Hilschmann, N. (1974) The primary structure of a monoclonal immunoglobulin L-chain of kappa-type, subgroup IV (Bence-Jones protein Len). A new subgroup of the kappa-type L-chain, *Hoppe-Seyler's Z. Physiol. Chem. 355*, 1164−1168.
19. O'Nuallain, B., Murphy, C. L., Wolfenbarger, D. A., Kennel, S., Solomon, A., and Wall, J. S. (2004) The amyloid-reactive monoclonal antibody 11-1F4 binds a cryptic epitope on fibrils and partially denatured immunoglobulin light chains and inhibits fibrillogenesis, in *Xth International symposium on Amyloid and Amyloidosis: from molecular dissection to therapeutics* (Grateau, G., Kyle, R. A., and Skinner, M., Eds.) pp 482−484, CRC Press, Boca Raton, FL, Tours, Loire Valley.
20. Benhar, I. (2001) Biotechnological applications of phage and cell display, *Biotechnol. Adv. 19*, 1−33.
21. Wang, L. F., and Yu, M. (2004) Epitope identification and discovery using phage display libraries: applications in vaccine development and diagnostics, *Curr. Drug Targets 5*, 1−15.
22. Morrison, K. L., and Weiss, G. A. (2001) Combinatorial alanine-scanning, *Curr. Opin. Chem. Biol. 5*, 302−307.
23. Wall, J., Schell, M., Murphy, C., Hrncic, R., Stevens, F. J., and Solomon, A. (1999) Thermodynamic instability of human lambda 6 light chains: correlation with fibrillogenicity, *Biochemistry 38*, 14101−14108.
24. O'Nuallain, B., Williams, A. D., Westermark, P., and Wetzel, R. (2004) Seeding specificity in amyloid growth induced by heterologous fibrils, *J. Biol. Chem. 279*, 17490−17499.
25. Wall, J., Murphy, C. L., and Solomon, A. (1999) In vitro immunoglobulin light chain fibrillogenesis, *Methods Enzymol. 309*, 204−217.
26. Naiki, H., and Gejyo, F. (1999) Kinetic analysis of amyloid fibril formation, *Methods Enzymol. 309*, 305−318.
27. Levine, H., 3rd. (1999) Qunatification of beta-sheet amyloid fibril structures with thioflavin T methods, *Methods Enzymol.* 274−284.
28. Thompson, J. D., Higgins, D. G., and Gibson, T. J. (1994) CLUSTAL W: improving the sensitivity of progressive multiple sequence alignment through sequence weighting, position-specific gap penalties and weight matrix choice, *Nucleic Acids Res. 22*, 4673−4680.
29. Bonnycastle, L. L. C., Menendez, A., and Scott, J. K. (2001) General phage methods, in *Phage Display: A Laboratory Manual* (Barbas, C. F., Burton, D. R., Scott, J. K., and Silverman, G. J., Eds.) Cold Spring Harbor Laboratory Press, New York.
30. Goldblatt, D. (1997) Simple solid phase assays of avidity, in *Immunochemistry 2: A pratical approach* (Johnstone, A. P., and Turner, M. W., Eds.) pp 31−51, Oxford University press, Oxford.
31. Taylor, W. R. (1986) The classification of amino acid conservation, *J. Theor. Biol. 119*, 205−218.
32. Kyte, J., and Doolittle, R. F. (1982) A simple method for displaying the hydropathic character of a protein, *J. Mol. Biol. 157*, 105−132.
33. Goldsteins, G., Persson, H., Andersson, K., Olofsson, A., Dacklin, I., Edvinsson, A., Saraiva, M. J., and Lundgren, E. (1999) Exposure of cryptic epitopes on transthyretin only in amyloid and in amyloidogenic mutants, *Proc. Natl. Acad. Sci. U.S.A. 96*, 3108−3113.
34. Linke, R. P., Zucker-Franklin, D., and Franklin, E. D. (1973) Morphologic, chemical, and immunologic studies of amyloid-like fibrils formed from Bence Jones Proteins by proteolysis, *J. Immunol. 111*, 10−23.
35. Franklin, E. C., and Pras, M. (1969) Immunologic studies of water-soluble human amyloid fibrils. Comparative studies of eight amyloid preparations, *J. Exp. Med. 130*, 797−808.
36. Yuan, F. F., Biffin, S., Brazier, M. W., Suarez, M., Cappai, R., Hill, A. F., Collins, S. J., Sullivan, J. S., Middleton, D., Multhaup, G., Geczy, A. F., and Masters, C. L. (2005) Detection of prion epitopes on PrP and PrP of transmissible spongiform encephalopathies using specific monoclonal antibodies to PrP, *Immunol. Cell Biol. 83*, 632−637.
37. Costa, P. M., Teixeira, A., Saraiva, M. J., and Costa, P. P. (1993) Immunoassay for transthyretin variants associated with amyloid neuropathy, *Scand. J. Immunol. 38*, 177−182.
38. Kabat, E. A., Wu, T. T., Perry, H. M., Gottesman, K. S., and Foeller, C. (1992) Sequence of proteins of immunological interest (NIH, Ed.) 5 ed., NIH.
39. Huber, R., and Steigemann, W. (1974) Two cis-prolines in the Bence-Jones protein Rei and the cis-pro-bend, *FEBS Lett. 48*, 235−237.
40. Ivanova, M. I., Sawaya, M. R., Gingery, M., Attinger, A., and Eisenberg, D. (2004) An amyloid-forming segment of beta2-microglobulin suggests a molecular model for the fibril, *Proc. Natl. Acad. Sci. U.S.A. 101*, 10584−10589.
41. Jahn, T. R., Parker, M. J., Homans, S. W., and Radford, S. E. (2006) Amyloid formation under physiological conditions proceeds via a native-like folding intermediate, *Nat. Struct. Mol. Biol. 13*, 195−201.
42. Huang, D. B., Chang, C. H., Ainsworth, C., Johnson, G., Solomon, A., Stevens, F. J., and Schiffer, M. (1997) Variable domain structure of kappa IV human light chain Len: high homology to the murine light chain McPC603, *Mol. Immunol. 34*, 1291−1301.
43. Rose, G. D., Gierasch, L. M., and Smith, J. A. (1985) Turns in peptides and proteins, *Adv. Protein Chem. 37*, 1−109.
44. Videau, L. L., Arendall, W. B., 3rd, and Richardson, J. S. (2004) The cis-Pro touch-turn: a rare motif preferred at functional sites, *Proteins 56*, 298−309.
45. Gellman, S. H. (1998) Minimal model systems for beta sheet secondary structure in proteins, *Curr. Opin. Chem. Biol. 2*, 717−725.

46. Russell, S. J., Blandl, T., Skelton, N. J., and Cochran, A. G. (2003) Stability of cyclic beta-hairpins: asymmetric contributions from side chains of a hydrogen-bonded cross-strand residue pair, *J. Am. Chem. Soc. 125*, 388−395.
47. Maynard, A. J., Sharman, G. J., and Searle, M. S. (1998) Origin of beta-hairpin stability in solution: structural and thermodynamic analysis of the folding of a model peptide supports hydrophobic stabilization in water, *J. Am. Chem. Soc. 120*, 1996−2007.
48. Demchuk, E., Bashford, D., and Case, D. A. (1997) Dynamics of a type VI reverse turn in a linear peptide in aqueous solution, *Fold. Des. 2*, 35−46.
49. Wu, W. J., and Raleigh, D. P. (1998) Local control of peptide conformation: stabilization of cis proline peptide bonds by aromatic proline interactions, *Biopolymers 45*, 381−394.
50. Yao, J., Dyson, H. J., and Wright, P. E. (1994) Three-dimensional structure of a type VI turn in a linear peptide in water solution. Evidence for stacking of aromatic rings as a major stabilizing factor, *J. Mol. Biol. 243*, 754−766.
51. Meng, H. Y., Thomas, K. M., Lee, A. E., and Zondlo, N. J. (2006) Effects of i and i+3 residue identity on cis-trans isomerism of the aromatic(i+1)-prolyl(i+2) amide bond: implications for type VI beta-turn formation, *Biopolymers 84*, 192−204.
52. Guruprasad, K., and Rajkumar, S. (2000) Beta-and gamma-turns in proteins revisited: a new set of amino acid turn-type dependent positional preferences and potentials, *J. Biosci. 25*, 143−156.
53. Balamurugan, B., Samaya Mohan, K., Ramesh, J., Roshan, M. N., Sumathi, K., and Sekar, K. (2005) SSEP-2.0: Secondary Structural Elements of Proteins, *Acta Crystallogr., Sect. D: Biol. Crystallogr. 61*, 634−636.
54. Li, L., Darden, T. A., Bartolotti, L., Kominos, D., and Pedersen, L. G. (1999) An atomic model for the pleated β-sheet structure of Aβ amyloid protofilaments, *Biophys. J. 76*, 2871−2878.
55. Meloen, R. H., Puijk, W. C., and Slootstra, J. W. (2000) Mimotopes: realization of an unlikely concept, *J. Mol. Recognit. 13*, 352−359.
56. Gevorkian, G., Petrushina, I., Manoutcharian, K., Ghochikyan, A., Acero, G., Vasilevko, V., Cribbs, D. H., and Agadjanyan, M. G. (2004) Mimotopes of conformational epitopes in fibrillar β-amyloid, *J. Neuroimmunol. 156*, 10−20.
57. Che, Y., and Marshall, G. R. (2006) Impact of cis-proline analogs on peptide conformation, *Biopolymers 81*, 392−406.
58. Che, Y., and Marshall, G. R. (2004) Impact of azaproline on Peptide conformation, *J. Org. Chem. 69*, 9030−9042.

BI701255M